Zirconium Tungstate (ZrW_2O_8)/Polyimide Nanocomposites Exhibiting Reduced Coefficient of Thermal Expansion

Lisa M. Sullivan and Charles M. Lukehart*

Department of Chemistry, Vanderbilt University, Nashville, Tennessee 37235

Received October 2, 2004. Revised Manuscript Received February 3, 2005

ZrW_2O_8 is obtained as microparticulate powder following traditional methods or as nanoparticulate powder using an inverse micelle sol−gel synthesis strategy. As-prepared ZrW_2O_8 powders, surface-derivatized with (3-aminopropyl)siloxy linker molecules, disperse well in BTDA-ODA polyamic acid resins to give thermally cured ZrW_2O_8/polyimide hybrid films showing good wetting of embedded ceramic particles. Measured CTE values of ZrW_2O_8/BTDA-ODA hybrid films containing 0−50 wt % (0−22 vol %) ceramic loading show a controlled reduction in thermal expansion with increasing ceramic content. Reduction in CTE is modeled best assuming mixed-law behavior with incorporation of an interfacial phase region. A 22 vol % ceramic loading gives a 30% (10 ppm/K) reduction of CTE. ZrW_2O_8/BTDA-ODA films containing 0.8 vol % (3 wt %) ceramic loading exhibit unusually low thermal expansion, although the significance of this observation remains to be confirmed.

Introduction

Ceramic/polymer composites, known collectively as ceramers, have been studied extensively as a class of inorganic/organic materials through which the physical and mechanical properties of a wide variety of organic polymers can be modified.[1,2] Polyimides have found much application as thin-film materials, and several ceramic/polyimide composites exhibit reduced coefficients of thermal expansion (CTEs) relative to the thermal expansion characteristics of the corresponding virgin polymer. Polyimide-based ceramers showing reduced CTEs have recently been prepared from organoclay/polyamic acid blends,[3−5] sol−gel-derived silica particulate/polyamic acid mixtures,[6,7] POSS (polyhedral oligomeric silsesquioxanes) or POSS-like/polyamic acid blends,[8,9] sol−gel incorporation of lanthanide precursor complexes into soluble polyimides,[10] or AlN/polyimide nanocomposites.[11,12] Because phase separation of the ceramic and polymer components should be minimized to ensure high-quality composite films and reduced CTE properties, multi-functional swelling agents or linker molecules capable of covalent binding across the ceramic/polymer interface are usually introduced into composite blends prior to polymer curing. Relatively high ceramic loading (ca. 30−50 wt % silica) is usually required to effect significant reduction in CTE.

Cubic zirconium tungstate, ZrW_2O_8, which can be prepared by a variety of methods[13−16] including sol−gel synthesis strategies,[15] has been used as an additive to control the thermal expansion properties of a variety of composite materials due to its relatively large isotropic, negative thermal expansion (CTE value of ca. -9×10^{-6}/K from 0.3 to 1443 K).[17−19] Admixture of ZrW_2O_8 into cement,[20] polyester, or epoxy polymers[21] gives composites exhibiting reduced thermal expansion properties. Reductions in CTE values from 94 to 56 ppm/K for ZrW_2O_8/polyester composites and from 54 to 18 ppm/K for ZrW_2O_8/epoxy composites have been observed for ceramic loadings ranging from 0 to 30 vol %.

Polyimide thin films are used in a variety of advanced applications, such as conformal coatings of electronic circuits or of reflective disks, in which thermal cycling leads to device degradation. Preparing ZrW_2O_8/polyimide thin films

---

* To whom correspondence should be addressed. E-mail: charles.m.lukehart@vanderbilt.edu.

(1) Wilkes, G. L.; Orier, B.; Huang, H.-H. *Polym. Prepr*. **1985**, *26*, 300.
(2) Huang, H.; Glaser, R. H.; Wilkes, G. L. In *Inorganic and Organometallic Polymers*; Zeldin, M., Wynne, K. J., Allcock, H. R., Eds.; ACS Symposium Series No. 360; American Chemical Society: Washington, DC, 1988; p 354.
(3) Hsu, S. L.-C.; Wang, U.; King, J.-S.; Jeng, J.-L. *Polymer* **2003**, *44*, 5533.
(4) Tyan, H.-L.; Leu, C.-M.; Wei, K.-H. *Chem. Mater.* **2001**, *13*, 222.
(5) Tyan, H.-L.; Liu, Y.-C.; Wei, K.-H. *Chem. Mater.* **1999**, *11*, 1942.
(6) Zhu, Z.-K.; Yang, Y.; Yin, J.; Qi, Z.-N. *J. Appl. Polym. Sci.* **1999**, *73*, 2977.
(7) Mascia, L.; Kioul, A. *Polymer* **1995**, *36*, 3649.
(8) Hsueh, H.-B.; Chen, C.-Y.; Wang, C.-C.; Chu, T.-J. *J. Appl. Polym. Sci.* **2003**, *89*, 2865.
(9) Phillips, S. H.; Blanski, R. L.; Svejda, S. A.; Haddad, T. S.; Lee, A.; Lichtenhan, J. D.; Feher, F. J.; Mather, P. T.; Hsiao, B. S. *Mater. Res. Soc. Symp. Proc.* **2001**, *628*, CC 4.6.1.
(10) Thompson, D. S.; Thompson, D. W.; Southward, R. E. *Chem. Mater.* **2002**, *14*, 30.
(11) Chen, X.; Gonsalves, K. E. *J. Mater. Res.* **1997**, *12*, 1274.
(12) Gonsalves, K. E.; Chen, X. *Mater. Res. Soc. Symp. Proc.* **1996**, *435*, 55.
(13) Closmann, C.; Sleight, A. W.; Haygarth, J. C. *J. Solid-State Chem.* **1998**, *139*, 424.
(14) Yang, P.; Zhao, D.; Margolese, D. I.; Chmelka, B. F.; Stucky, G. D. *Nature (London)* **1998**, *396*, 152.
(15) Kameswari, U.; Sleight, A. W.; Evans, J. S. O. *Int. J. Inorg. Mater.* **2000**, *2*, 333.
(16) Lind, C.; Wilkinson, A. P. *J. Sol.-Gel Sci. Technol.* **2002**, *25*, 51.
(17) Mary, T. A.; Evans, J. S. O.; Vogt, T.; Sleight, A. W. *Science* **1996**, *272*, 90.
(18) Evans, J. S. O.; David, W. I. F.; Sleight, A. W. *Acta Crystallogr., Sect. B* **1999**, *B55*, 333.
(19) Duan, N.; Kameswari, U.; Sleight, A. W. *J. Am. Chem. Soc.* **1999**, *121*, 10432.
(20) Kofteros, M.; Rodriguez, S.; Tandon, V.; Murr, L. E. *Scr. Mater.* **2001**, *45*, 369.
(21) Shi, J. D.; Pu, Z. J.; Wu, K.-H.; Larkins, G. *Mater. Res. Soc. Symp. Proc.* **1997**, *445*, 229.

10.1021/cm0482737 CCC: $30.25

having controlled, reduced thermal expansion would, therefore, be of practical interest. We now report the synthesis of surface-derivatized micro- and nanoparticulate ZrW_2O_8, and the fabrication of ZrW_2O_8/BTDA-ODA polyimide thin films (where BTDA = 3,3′,4,4′-benzophenonetetracarboxylic dianhydride and ODA = 4,4′-oxydianiline) in which the embedded ceramic particles appear to be in close contact with the polymer phase. CTE values of the resulting ceramer can be reduced by 30% in a controlled fashion as the ZrW_2O_8 loading is increased from 0 to 50 wt % (or 0−22 vol %).

Experimental Section

Reagents and General Methods. Prepurified nitrogen gas (A.L. Gas, Inc.) was passed through a drying column containing Drierite ($CaSO_4$) prior to use. Reagent grade organic solvents were purchased from Sigma-Aldrich Chemical Co., Inc. Zirconium dichloride oxide hydrate and ammonium metatungstate hydrate were purchased from Strem Chemical Co., Inc. Triton N-101, KCN, ninhydrin, and tetraethylammonium bromide were purchased from Sigma-Aldrich Chemical Co., Inc. 3-Aminopropyltrimethoxysilane was purchased from Gelest, Inc.

X-ray diffraction (XRD) scans were obtained using a Scintag X_1 θ/θ automated powder X-ray diffractometer with a Cu target, a Peltier-cooled solid-state detector, and zero-background, Si(510) sample support. Scans at elevated temperature were recorded using a Buehler high-temperature attachment.

Samples for transmission electron microscopy (TEM) imaging were prepared by placing a drop of a ceramic/acetone suspension onto a holey carbon-coated, copper grid followed by evaporation of the acetone. Average particle size was determined by manually measuring over 100 particles from bright-field micrographs recorded on a Philips CM20T TEM operating at 200 kV.

Samples for scanning electron microscopy (SEM) imaging were prepared by evaporating Au on the surface of the sample with a Pelco model 3 sputter and coater. The samples were mounted on carbon tape before investigation using a Hitachi S-4200 SEM.

Thermal treatments were conducted inside a quartz tube under continuous air flow using a one-foot Lindberg/Blue tube furnace. The temperature was ramped at 20 °C/min to 600 °C and held for 10 h.

Thermogravimetric analysis (TGA) was conducted using a TA Instrument Hi-Res TGA 2950 Thermogravimetric Analyzer. The scans were collected under a flow of $N_{2(g)}$ at a heating rate of 10 °C/min to 600 °C.

Surface-area measurements were performed using a NOVA-1000 Gas Sorption Analyzer (Quantachrome). Surface areas were calculated from adsorption isotherms using the Brunauer−Emmett−Teller method. Bulk elemental analyses were performed by Atlantic Microlab, Inc., Norcross, GA.

Preparation of Microparticulate ZrW_2O_8. ZrW_2O_8 was prepared according to a literature procedure with slight modification.[13] Specifically, aqueous stock solutions of 0.08 M ammonium metatungstate hydrate and 0.50 M zirconium dichloride oxide hydrate were prepared. Fifty milliliters of each of these solutions were simultaneously added dropwise with stirring to a 500 mL round-bottom flask containing 25 mL of distilled water. Upon addition, an immediate viscous, white precipitate formed that hindered the stirring motion. After 30 min, the suspension achieved a less viscous consistency that allowed stirring to continue. This solution was stirred under ambient conditions for 10 h. A solution of 125 mL of 6 M HCl was then added to the flask, and the reaction was refluxed for 48 h. The reaction solution was cooled to room temperature and was centrifuged to yield a white precipitate. The precipitate was washed two times with 15.0 mL of distilled water and was aged at room temperature open to air for 7 days. Aging produced a light green-white precipitate that was calcined under a flow of air at 600 °C for 10 h. This procedure produced ca. 13 g (22.0 mmol) of ZrW_2O_8 as a dry green-white powder. Elemental analysis of as-prepared microparticulate ZrW_2O_8: 0.16% C, 0.25% H, and 0.11% N.

Preparation of Nanoparticulate ZrW_2O_8. Nanoparticulate ZrW_2O_8 was prepared by a combination of sol−gel processing and inverse micelle synthesis.[22] The following chemicals were added to a 500 mL round-bottom flask with rapid stirring: 158 mL (1.46 mol) of cyclohexane, 6.5 mL (0.052 mol) of n-hexanol, and 20.0 mL (0.067 mol) of Triton N-101. In a small vial, 3.8 g (1.29 mmol) of ammonium metatungstate hydrate was dissolved in 6.5 mL of distilled water to yield a clear, colorless solution. In a separate vial, 2.6 g (16.3 mmol) of zirconium dichloride oxide hydrate was dissolved in 2.5 mL of distilled water to produce a clear, colorless solution. These two aqueous solutions were mixed by simultaneous dropwise addition to a small vial producing a clear, colorless premix solution. This premix solution was added dropwise to the aforementioned 500 mL reaction flask with rapid stirring. Immediately, the reaction solution turned turbid. After 10 min of reaction, the reaction consisted of a clear, colorless liquid phase and a white precipitate. After ∼1 h of reaction, the precipitate dissolved, and the entire reaction solution became clear and colorless. After 4 h of reaction, 100 mL of absolute ethanol was added to the reaction flask, and the reaction solution immediately became a white, turbid suspension. This suspension was stirred for 1 h and was then centrifuged to yield a white, gellike precipitate. The gellike precipitate was suspended and washed in 15 mL of absolute ethanol five times and was then transferred to a 500 mL round-bottom flask. To aid in the transfer, 125 mL of distilled water was used to form a slurry, and 125 mL of 6 M HCl was also added to the round-bottom flask. The reaction solution was allowed to reflux for 48 h. The flask was then cooled to room temperature, and the white solution was centrifuged to yield a white precipitate. The precipitate was washed two times with 15 mL of water and aged at room temperature open to air for 7 days. The aged precipitate was calcined under a flow of air at 600 °C for 10 h to yield a yellowish-white precipitate. This procedure produced ca. 4.3 g (7.33 mmol) of ZrW_2O_8 as a yellowish-white, dry powder. Elemental analysis (wt %) of as-prepared nanoparticulate ZrW_2O_8: 0.20% C, 0.16% H, and 0.12% N.

Surface Derivatization of ZrW_2O_8 Particulates. To enhance the dispersion properties of ceramic particles prior to surface derivatization, samples of ZrW_2O_8 were sonicated in a solution of dimethylacetamide, DMAC, using a Branson Ultrasonics 450 Analogue ultrasonifier. The ceramic samples were sonicated at 30 W of power emission for 6 h in a suspension of 150 mL of DMAC. Following sonification, DMAC was removed with centrifugation. The precipitate was suspended and washed three times with 15 mL of distilled tetrahydrofuran, THF, and three times with 15 mL of distilled ether. The resulting ceramic powder was dried and stored under vacuum overnight. A 100 mL round-bottom flask containing a stirring bar was assembled and was purged with $N_{2(g)}$. A 7.4 g (12.6 mmol) sample of sonicated ZrW_2O_8 powder was transferred to the flask under a $N_{2(g)}$ purge. Under flowing $N_{2(g)}$, 37.4 mL of distilled 3-aminopropyltrimethoxysilane was syringed into the 100 mL reaction flask. The reaction mixture was allowed to stir at 50 °C under $N_{2(g)}$ for 15.5 h. The contents of the reaction flask were then centrifuged to yield a precipitate that was washed five times with 15 mL of distilled THF and three times with 15 mL of distilled

---

[22] Johnson, S. A.; Ollivier, P. J.; Mallouk, T. E. *Science* **1999**, *283*, 963−965.

ether. The sample was dried under vacuum at room temperature overnight. Elemental analysis (wt %) of surface-derivatized microparticulate ZrW_2O_8: 0.36% C, 0.26% H, and 0.17% N. Elemental analysis (wt %) of surface-derivatized nanoparticulate ZrW_2O_8: 0.54% C, 0.16% H, and 0.24% N.

Primary Amine Analysis Using the Ninhydrin Reaction. The number density of free amino groups on surface-derivatized ZrW_2O_8 was determined using slight modification of the known ninhydrin reaction method.[23] Ninhydrin analysis of surface-derivatized microparticulate ZrW_2O_8 gave the following result: 44.1 μmol NH_2/g ceramic powder. Ninhydrin analysis of surface-derivatized nanoparticulate ZrW_2O_8 gave the following result: 97.0 μmol NH_2/g ceramic powder.

Polyimide Thin-Film Fabrication and Characterization. Polyimide thin-film fabrication was performed at Physitron, Inc. (Hunstsville, AL). Virgin polymer and ceramer thin-film characterization was performed at NASA Langley Research Center. Thermal expansion measurements were performed using a TA Instruments 2940 TMA from room temperature to 150 °C at 2.5 °C/min heating rate. Glass-transition (T_g) measurements were determined by differential scanning calorimetry (DSC), while 10% weight-loss temperature measurements were recorded by TGA. Ceramer thin-film specimens were fabricated following three different processing modes, as described below.

Dianhydride Prepolymerization Processing (Mode 1). A 50-g resin synthesis was processed according to the following procedure. To 5.555 g of the dianhydride copolymerization monomer, BTDA, contained in a dry reaction bottle was added 42.284 g of NMP. The mixture was stirred under a N_2 atmosphere until a solution was obtained. A 0.2780 g sample of surface-derivatized ZrW_2O_8 powder was then added to this solution and allowed to mix for 15 min. A 3.449 g portion of solid 4,4′-ODA was added, and the combined reaction mixture was stirred under nitrogen for 15 h using a magnetic stirrer. The resulting ceramic/polyamic acid resin suspension was stored under nitrogen at 10 °C to inhibit further curing and polyimide formation. The resin obtained had low viscosity indicating a low molecular weight. A high level of ceramic material quickly precipitated out of this suspension, possibly indicating poor covalent bonding at the particle/polymer interface. Nanocomposite resins were made using only 3 and 6 wt % loading of ZrW_2O_8.

Diamine Prepolymerization Processing (Mode 2). This technique was very similar to dianhydride prepolymerization processing, except that functionalized ZrW_2O_8 particles were reacted initially with the diamine copolymerization monomer, 4,4′-ODA, dissolved in NMP. A calculated amount of BTDA was then added to stoichiometrically balance the NH_2 groups of the BTDA and the functionalized ceramic particles. To 3.449 g of 4,4′-ODA in a dry reaction bottle was added 42.284 g of NMP, and the mixture was stirred under N_2 until the diamine was dissolved. Next, 0.278 g of surface-functionalized ZrW_2O_8 was added to the reaction vessel, and the resulting mixture was mixed for 15 min. A 5.555 g portion of BTDA was added to the mixture, and the mixture was stirred for 15 h under N_2. The resulting ceramic/polyamic acid resin mixture was stored under N_2 at 10 °C. The material provided by this technique had a much higher viscosity than the dianhydride prepolymerization synthesis and exhibited a high level of particulate suspension and dispersion. However, at higher loading levels of ceramic additive, the viscosity of the resin dropped significantly, indicating again a possible premature polymer chain termination was occurring. Nanocomposite resins were prepared using 3%, 6%, and 10% weight loading of microparticulate ZrW_2O_8 and 3% and 6% weight loading of nanoparticlulate ZrW_2O_8.

Postpolymerization Ceramer Processing (Mode 3). Postpolymerization synthesis techniques were also investigated as a means to produce a hybrid material. Excess dianhydride (BTDA) was added to preprepared polyamic acid resin. This process was investigated to develop a method that kept high molecular weight polymer chains throughout the hybrid material synthesis. To 3.449 g of 4,4′-ODA in a dry reaction bottle was added 42.292 g of NMP under N_2, and the mixture was stirred until the diamine dissolved. A 5.556 g portion of BTDA was added to the resulting solution and was mixed overnight. An additional 0.006 g portion of solid BTDA was added to the obtained polyamic acid resin, and the resin was mixed for 2 h. A 0.2780 g sample of surface-derivatized ZrW_2O_8 was then added to the resin, and the resulting mixture was stirred for 6 h. The final mixture was stored at 10 °C. In some reactions, the ceramic powder was added with additional solvent to thin the polyamic acid and to provide greater particle mobility within the resin solution. Also, the particles were sonicated in the solvent for a short amount of time to increase particulate dispersion. After sonification, the ceramic/NMP solution was added to the polyamic acid, and the final resin solution was mixed using an ultrasonic bath. Ceramic/resin mixtures containing 3, 6, 25, and 50 wt % ceramic loadings were prepared.

Polyimide Film Casting, Drying, Curing, and Releasing. Glass substrates were cleaned with 2-propanol several times to ensure that all of the dust was removed from the glass. The substrates were dried with pressurized air, wiped with a static free brush to further ensure no dust was present, and then placed on a heat pad in a container designed as an ultra-clean environment for casting films. Nitrogen gas was flowed through the container to ensure low humidity conditions as the films dried. Once the resin (or creamer/resin hybrid mixture) was poured onto the substrate, a clean Mayer rod was used to draw the resin down the substrate to fabricate the desired film. The Mayer rod was used to ensure that the films were of uniform thickness (i.e., approximately 25 μm). Cast films were heated slowly to and dried at 80 °C and then were allowed to cool. The dried films were then cured. While still on the substrate, the films were put into an oven under a nitrogen purge container. The container provided a constant convective current of nitrogen gas over the film, guaranteeing the continuous removal of water released from the imidization reaction and preventing oxidation of the film. The oven was gradually heated to 350 °C (10 °C/min) and was held for 1 h at that temperature to complete the imidization process. The oven was then allowed to cool slowly. The nitrogen flow was maintained throughout cooling, as a precautionary measure to ensure that no oxidation would occur. Once the films had cooled to room temperature, the substrate was removed from the nitrogen purge container and was placed in a tub of distilled water. The water causes the film to release from the glass over a period of 3 h, and the resulting film floats to the surface. The film was then dried, trimmed, and prepared for property evaluation. Property evaluation under conditions of thermal cycling is anticipated in future work.

Results and Discussion

For this study, ZrW_2O_8 powders have been prepared by two methods. Microparticulate ZrW_2O_8 is prepared by co-condensation of ammonium metatungstate hydrate and zirconium dichloride oxide hydrate solutions following the previously reported multi-day synthesis procedure, shown in eq 1.[13] To prepare ZrW_2O_8 of smaller particle size more amenable for dispersion in organic polymer resin, the initial

---

(23) Sarin, V. K.; Kent, S. B. H.; Tam, J. P.; Merrifield, R. B. *Anal. Biochem.* **1981**, *117*, 147−157.

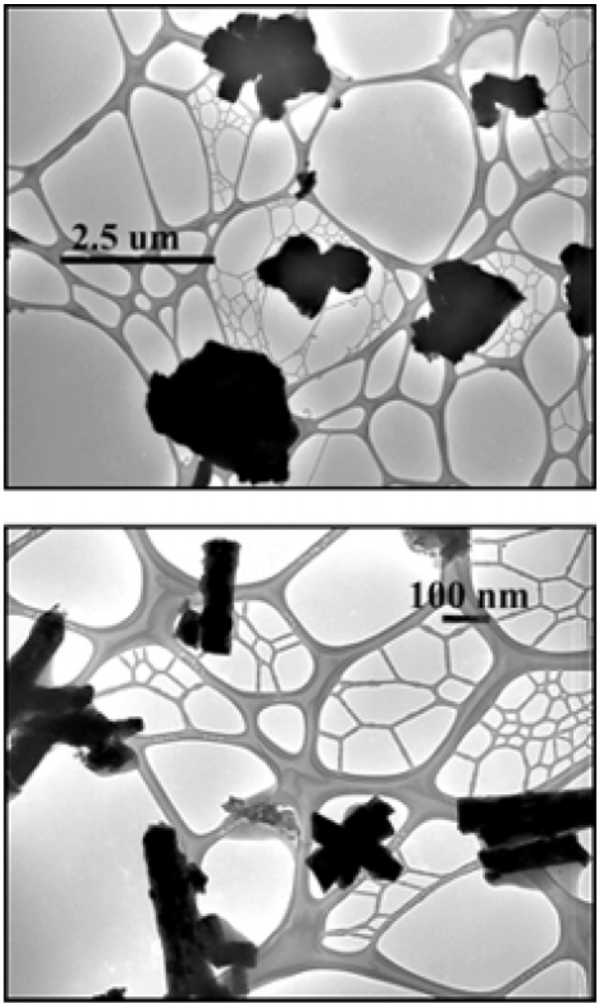

Figure 1. TEM micrographs of microparticulate (upper) and nanoparticulate (lower) ZrW_2O_8.

co-condensation of the W and Zr reactant solutions is confined to aqueous regions formed within inverse micelles. The resulting sol−gel product is then subjected to the same acid treatment and aging procedures shown in eq 1. TEM micrographs of ZrW_2O_8 products obtained from these two different synthesis protocols are shown in Figure 1. Micrometer-scale ZrW_2O_8 particles (dimensions of 500 nm to >1 μm) having very heterogeneous shapes are obtained from the traditional synthesis method, while submicrometer particles are formed when sol−gel condensation is permitted to occur within inverse micelles. In the latter case, the nanoparticulate ceramic product consists of predominantly parallelepiped particles (dimensions of ca. 200 nm × 200 nm × 100 nm).

$$[NH_4]_6[W_{12}O_{39}]\bullet xH_2O \;+\; 6\,ZrOCl_2\bullet yH_2O \xrightarrow[10\text{ h}]{\text{stir}} \xrightarrow[\Delta,\ 2\text{ d}]{6M\text{ HCl}} \xrightarrow[7\text{ d}]{\text{age}} \begin{array}{c} ZrW_2O_7(OH)_2\bullet 2H_2O \\ \text{air}\Big\downarrow 600\ \ \text{C, 10 h} \\ ZrW_2O_8 \end{array} \quad (1)$$

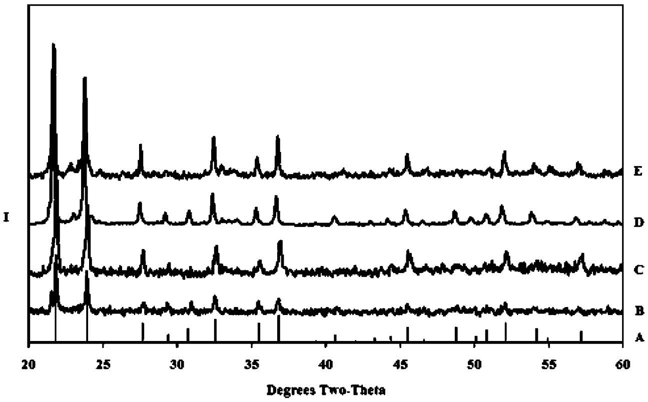

Figure 2. XRD scans (Cu Kα radiation) of pure ZrW_2O_8 (scan A, PDF Card #13-557), microparticulate ZrW_2O_8 (scan B at 25 °C; scan C at 475 °C), and nanoparticulate ZrW_2O_8 (scan D at 25 °C; scan E at 475 °C).

Low-resolution XRD scans of the micro- and nanoparticulate ZrW_2O_8 product powders are shown in Figure 2 at both room temperature and at 475 °C along with the XRD line pattern of pure α-cubic ZrW_2O_8. The slight shift to higher 2θ observed in both XRD patterns with increasing temperature is consistent with materials exhibiting a negative CTE. From cell constants derived at these two temperatures, CTE values of -5 ± 2 and -4 ± 2 ppm/K can be calculated for the micro- and nanoparticulate products, respectively. Although no attempt was made to improve either the accuracy or the precision of these calculated CTE values, these XRD scans confirm the successful formation of cubic ZrW_2O_8 by either synthesis method.

To enhance the dispersibility of ZrW_2O_8 ceramic particles in polyamic acid resin, as-prepared micro- and nanoparticulate ZrW_2O_8 powders are surface-derivatized with reactive linker molecules capable of binding to functional groups present in polyamic acid resins during thermal curing. Sol−gel reaction of surface M−OH groups present on as-prepared ZrW_2O_8 powders with neat 3-aminopropyltrimethoxysilane leads to covalent attachment of 3-aminopropylsiloxy linker molecules at surface sites on the ceramic particles. Subsequent amidation or condensation reactions between these pendant amino groups and polyamic acid resin during polymer film curing ensures both good wetting of the ceramic particles by the polymer component and a ceramic/polymer interface of high integrity.

Successful surface derivatization of as-prepared ZrW_2O_8 particles with 3-aminopropylsiloxy linker molecules is confirmed by elemental analysis data and by quantitative determination of the presence of free amino groups via ninhydrin analysis. These analyses are consistent with (linker molecule)/ZrW_2O_8 compositions of ca. 1:40 and 1:20 for the microparticulate and nanoparticulate ZrW_2O_8 powders, respectively. The nanoparticulate powder is expected to have a greater linker molecule content due to its higher surface area (13 m^2/g for microparticulate powder and 18 m^2/g for nanoparticulate powder). Quantification of the presence of surface amino groups using standard acid-uptake analysis is not possible. In acidic solution (pH = ca. 3), surface linker molecules undergo hydrolytic cleavage affording ceramic powders lacking nitrogen content (as determined by elemental analysis).

TGA scans of surface-derivatized micro- and nanoparticulate ZrW_2O_8 (see Supporting Information) reveal a two-step weight-loss curve. A well-defined mass loss of ca. 1 wt % centered at 133 °C is observed for both samples and is consistent with loss of water. From 200 to 450 °C, a single, broad mass-loss event assigned to linker molecule degradation is also observed for both samples. This mass loss is more articulated for the nanoparticulate sample and is centered at ca. 366 °C. Mass losses of 0.12 and 0.20 wt % are observed in this temperature range for the micro- and nanoparticulate powders, respectively, consistent with greater incorporation of linker molecules in the nanoparticulate sample. However, the expected mass fraction of linker molecule content (<0.5 wt %) is sufficiently small that quantification by TGA may not be reliable.

Virgin polymer and ZrW_2O_8/polyimide thin films have been prepared using BTDA-ODA as the polymer component. Virgin thin films are prepared by reacting anhydrous BTDA dianhydride monomer with ODA diamine monomer in NMP solution under nitrogen to form the corresponding polyamic acid resin. The resulting resin is cast onto a clean glass surface using a Mayer rod draw technique to give a uniform film ca. 25 micrometers thick. Under slow heating and a flow of nitrogen gas, the cast films are dried at 80 °C and then are thermally cured at 350 °C. The cured polyimide film is released from the glass substrate by soaking in water.

Virgin BTDA-ODA thin films prepared by the above procedure are of good quality (see Supporting Information). DSC and TGA curves reveal a T_g value of 287 °C, indicating essentially complete polymer curing and excellent chemical stability with a 10 wt % loss temperature of 513 °C. A TMA curve shows highly linear thermal expansion from 65 to 100 °C, so this temperature range has been used to determine CTE values of all thin-film specimens.

Ceramer films have been prepared following this same procedure but with introduction of the surface-derivatized ZrW_2O_8 component at three different points: (1) pre-reaction of surface-derivatized ZrW_2O_8 with BTDA in NMP solution (mode 1), (2) pre-reaction of surface-derivatized ZrW_2O_8 with ODA in NMP solution (mode 2), or (3) pre-reaction of polyamic resin with a calculated amount of BTDA to give anhydride chain termination followed by addition of surface-derivatized ZrW_2O_8 (mode 3).

Ceramer films prepared using either surface-derivatized or underivatized ZrW_2O_8 powders have very different apparent quality. As shown in Figure 3, SEM micrographs of ceramer films prepared using surface-derivatized ZrW_2O_8 reveal an intimate ceramic/polymer interface within the resolution of the image, while images of ceramer films using underivatized ZrW_2O_8 powder reveal poor ceramic/polymer wetting with significant void space surrounding each ceramic particle. For this study, only the higher quality ZrW_2O_8/polyimide thin films fabricated with surface-derivatized ceramic particles have been used.

Representative DSC, TGA, and TMA curves for ZrW_2O_8/polyimide thin-film specimens fabricated using surface-derivatized microparticulate ZrW_2O_8 at 50 wt % ceramic loading reveal a T_g value of 284 °C, a 10% weight loss temperature of 553 °C, and highly linear thermal expansion from 65 to 100 °C (see Supporting Information). The close correspondence between the film properties of virgin polymer and those of ceramer specimens indicates comparable film quality for both types of films.

Property data, including CTE values, measured for a variety of ZrW_2O_8/BTDA-ODA thin film samples are provided in Table 1. Figure 4 shows a plot of CTE experimental values (average of all data) versus vol % ceramic loading (data points showing esds) as well as continuous curves showing the compositional dependence of CTE values calculated assuming mixed-law behavior (— — —) or the Shi (—) and Turner models (- - - -). Composite CTE values, α_C, following mixed-law behavior scale as the CTE of each phase, α_M (matrix) and α_F (filler), weighted by the respective volume fractions, ϕ_M and ϕ_F, of each phase, eq 2. Shi's model, eq 3, incorporates into the mixed-law model an interphase region caused by matrix/filler interaction.[24] When no such interaction is present, mixed-law behavior is predicted. The size of this interphase

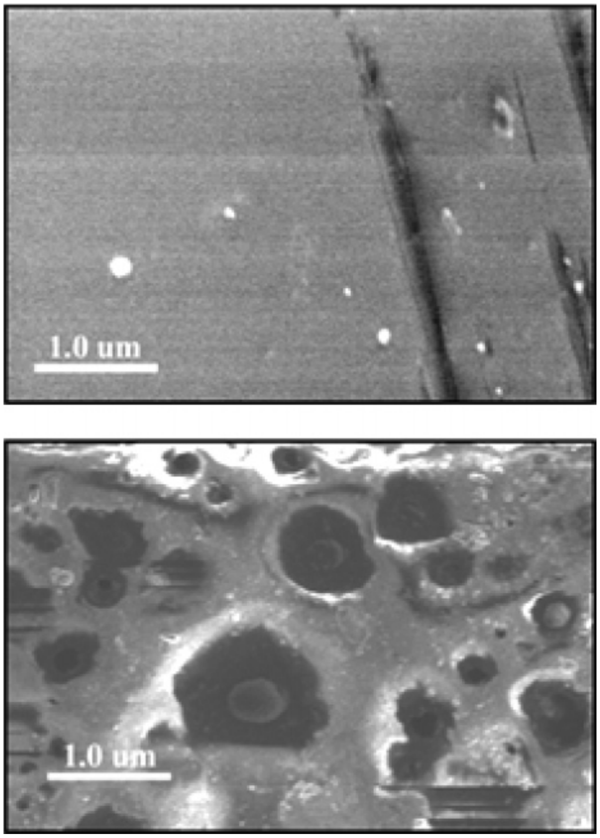

Figure 3. SEM micrographs of ZrW_2O_8/BTDA-ODA polyimide thin films fabricated using surface-derivatized (top) or underivatized (bottom) ZrW_2O_8 powder as the ceramic component. Note the presence of significant void space surrounding ceramic particles in the lower micrograph. Partial charging of SEM samples brightens the contrast of some ceramic particles.

Table 1. Property Data Measured for a Set of ZrW_2O_8/BTDA-ODA Thin Films[a]

ZrW_2O_8 load (wt % [vol %])	ZrW_2O_8 particle size	synthesis mode	CTE (ppm/K)	T_g (°C)	10 wt % loss temp (°C)
0 [0]		virgin	33 ± 3	287	513
3 [0.8]	micro	3	26 ± 2	285	513
3 [0.8]	micro	2	26 ± 1	285	514
3 [0.8]	nano	2	27 ± 3	284	522
6 [1.7]	micro	1	32 ± 1	274	507
6 [1.7]	micro	2	33 ± 2	287	494
6 [1.7]	nano	2	30 ± 1	284	527
10 [3]	micro	2	31 ± 3	283	527
25 [8]	micro	3	26 ± 2	284	548
50 [22]	micro	3	23 ± 2	284	553

[a] Errors (esds) are calculated from data measured on 3−5 duplicate samples.

---

(24) Vo, H. T.; Todd, M.; Shi, F. G.; Shapiro, A. A.; Edwards, M. *Microelectron. J.* **2001**, *32*, 331.

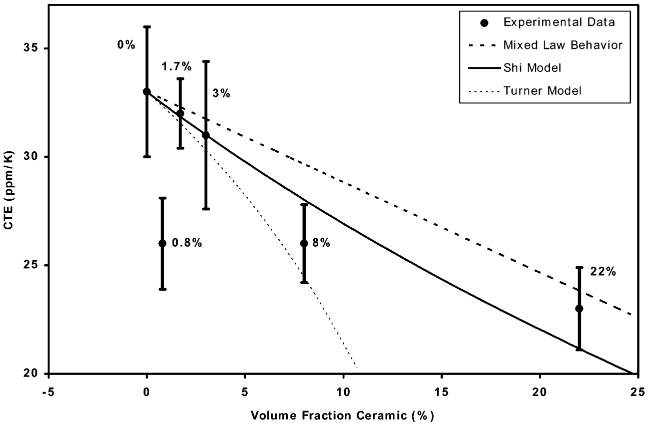

Figure 4. Plot of experimental CTE values versus ceramic loading (vol %) for ZrW_2O_8/BTDA-ODA thin films along with curves representing CTE values calculated assuming mixed-law behavior (− − −), Shi's model (−), or Turner's model (- - - -).

region can be calculated from the values of K_0 and K_1 that are determined by fitting eq 3 to experimental CTE data. For the curve shown in Figure 4, iterative curve fitting gives $K_0 = 0.98$ and $K_1 = -19$. In Turner's model, eq 4, composite CTE values depend on the volume fraction of each component and the bulk modulus of the matrix and filler material, K_M and K_F, respectively.[25] For the curve shown, bulk moduli values of 4.45 GPa for the polyimide phase and of 74.4 GPa for the ZrW_2O_8 ceramic phase have been used.[26]

$$\alpha_C = \alpha_M\phi_M + \alpha_F\phi_F \tag{2}$$

$$\alpha_C = [\alpha_M\phi_M + \alpha_F\phi_F + K_0\phi_F\phi_M(\alpha_F + \alpha_M) + K_0\phi_F\phi_M K_1]/(1 + K_0\phi_F\phi_M) \tag{3}$$

$$\alpha_C = [(1 - \phi_F)K_M\alpha_M + \phi_F K_F\alpha_F]/[(1 - \phi_F)K_M + \phi_F K_F] \tag{4}$$

Although the effect of each experimental parameter on film thermal expansion has not been fully investigated, the following observations can be made: (1) CTE values do not strongly depend on either the processing mode or the ZrW_2O_8 average particle size; (2) CTE values decrease with increasing ceramic loading; and (3) the CTE value is anomalously low for thin films containing 0.8 vol % (3 wt %) ceramic loading. Excluding this latter data point, the observed CTE values fall within 1.5 esd of the values expected assuming mixed-law behavior with even a better fit provided by Shi's model. Assuming an average ceramic nanoparticle radius of 100 nm, Shi's model predicts an interphase polymer region of ca. 30 nm thickness. Given that the chain length of a BTDA-ODA repeating unit is ca. 2 nm, structural distortion of the polyimide phase due to ZrW_2O_8/polyimide interfacial binding is predicted to extend over ca. 15 repeating units into the polymer matrix. Turner's model gives poor prediction of CTE for these ZrW_2O_8/polyimide nanocomposites due to the large bulk modulus and negative CTE of ZrW_2O_8.

The CTE value of 26 ± 2 ppm/K for ceramer specimens containing 0.8 vol % (3 wt %) ceramic loading is based on 10 measurements from specimens prepared as three independent batches of film. This experimental value is lower than the CTE value expected assuming either mixed-law behavior or Shi's model by nearly 3 standard deviations. A model rationalizing this unexpected observation, if statistically significant, remains elusive. An overall 30% reduction in the CTE of BTDA-ODA in going from 0 to 50 wt % (0−22 vol %) ZrW_2O_8 loading is comparable to reductions in CTE observed for ZrW_2O_8/polyester or epoxy composites.[21]

Conclusions

ZrW_2O_8 powders, prepared by solution-phase condensation or inverse-micelle methods and surface-derivatized with 3-aminopropylsiloxy linker molecules, form polyimide thin-film hybrid composites of good quality. Increasing the ceramic loading from 0 to 22 vol % gives controlled reduction in composite CTE values of up to 30% (10 ppm/K). The overall dependence of CTE reduction on ceramic loading is modeled best assuming mixed-law behavior with incorporation of an interfacial phase region. It is suggested that ZrW_2O_8/polyimide hybrid composites could be used as the polymer component of more traditional ceramer blends to achieve even greater reductions in CTE.

Acknowledgment. Portions of this research were funded through a Phase I research grant provided by Physitron, Inc., of Huntsville, AL. Property measurements provided by the NASA Langley Research Center are also gratefully acknowledged.

Supporting Information Available: Thermogravimetric analysis curves, DSC curves, TMA scans, and a typical EDS spectrum (PDF). This material is available free of charge via the Internet at http://pubs.acs.org.

CM0482737

---

(25) Wong, C. P.; Bollampally, R. S. *J. Appl. Polym. Sci.* **1999**, *74*, 3396.
(26) Drymiotis, F. R.; Ledbetter, H.; Betts, J. B.; Kimura, T.; Lashley, J. C.; Migliori, A.; Ramirez, A. P.; Kowach, G. R.; Van Duijin, J. *Phys. Rev. Lett.* **2004**, *93*, 025502.